IEEE Access
Multidisciplinary ⋮ Rapid Review ⋮ Open Access Journal

Received 24 July 2023, accepted 4 August 2023, date of publication 10 August 2023, date of current version 16 August 2023.

Digital Object Identifier 10.1109/ACCESS.2023.3304238

RESEARCH ARTICLE

Multiple Open Switch Fault Diagnosis of Three Phase Voltage Source Inverter Using Ensemble Bagged Tree Machine Learning Technique

CHUKWUEMEKA N. IBEM[1], (Member, IEEE), MOHAMED E. FARRAG[1], (Member, IEEE), AHMED A. ABOUSHADY[1], (Senior Member, IEEE), AND SHERIF M. DABOUR[1,2], (Senior Member, IEEE)

[1]Department Electrical and Electronic Engineering, School of Computing, Engineering and Built Environment (SCEBE), Glasgow Caledonian University, G4 0BA Glasgow, U.K.
[2]Department of Electrical Power Engineering, Faculty of Engineering, Tanta University, Tanta 31733, Egypt

Corresponding author: Chukwuemeka N. Ibem (Chukwuemeka.ibem@gcu.ac.uk)

ABSTRACT Three-phase converters based on insulated-gate bipolar transistors (IGBTs) are widely used in various industrial applications. Faults in IGBTs can significantly affect the operation and safety of the power electronic equipment and loads. It is critical to accurately detect power inverter faults as soon as they occur to ensure system availability and high-power quality. This study provides a novel integration of signal and data-driven fault-diagnosis approaches for detecting open-circuit switch faults in three-phase inverters. The proposed technique uses the average root-mean-square (RMS) ratio of the phase current as the key extraction feature. This feature can be used to estimate the fault types and faulty switches (es) irrespective of changes in the running load. Ensemble-bagged machine learning classification was used to accurately predict the faulty switch of the inverter. The results demonstrate the ability of the proposed fault diagnosis technique to identify single-, double-, and triple-switch fault (s). The experimental results also attested to the simulation of multiple fault diagnosis. A unique feature of this technique is its ability to estimate faulty switches under various inverter-operating conditions.

INDEX TERMS Ensemble bagged, fault diagnosis, open-circuit fault, voltage source inverter, IGBT.

I. INTRODUCTION

Voltage Source Inverters (VSIs) play a vital role in the contemporary industry and energy sectors, with applications extending from induction motor drives to renewable energy integration and power-efficient systems [1]. The failure of these devices can lead to operational disruption and consequential economic loss. Research on motor drives and renewable energy conversion systems reveals that VSIs are particularly susceptible to faults and exhibit a high failure rate, as depicted in Fig.1 [2].

Insulated Gate Bipolar Transistors (IGBTs) are one of the common VSI components that are especially prone to faults, accounting for 38% of VSI failures [3], [4]. These can be categorized into short-circuit (SC), gate-drive malfunction, and open-circuit (OC) faults, often resulting from environmental conditions, thermal stress, or ageing [1], [5].

Short-circuit faults can inflict immediate and severe damage, necessitating protective mechanisms such as fuses and circuit breakers [4]. On the other hand, open-circuit faults may not cause instant damage but can degrade the power quality of the inverter output, potentially harming other system components. Over time, open-circuit faults can prompt a total system shutdown [6]. Hence, it is essential to detect open- and short-circuit faults promptly to prevent extensive damage to the converter system.

Fault diagnosis (FD) is a vital reliability-cantered tool used to identify, classify, and locate faults, which in turn reduces the downtime of the inverter system. Over the years, considerable research has been conducted to investigate the performance of power switches under open circuit conditions.

The associate editor coordinating the review of this manuscript and approving it for publication was Pinjia Zhang.

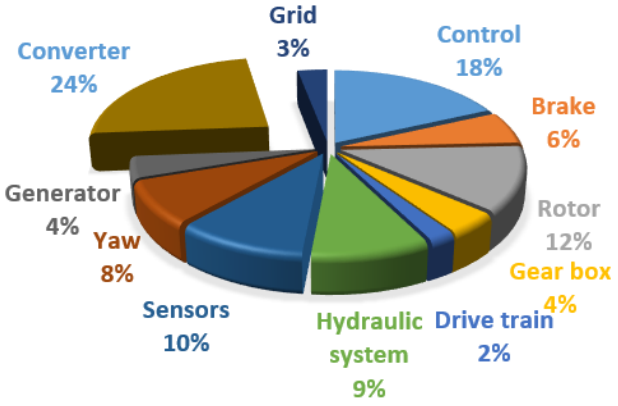

FIGURE 1. Failure rate of wind energy conversion system components [7].

This has resulted in the development of fault diagnosis and fault-tolerant techniques.

Fig.2 shows the common open-circuit faults in a VSI. These faults include gate driver malfunctions, open-switch faults, and diode open faults [5], [8]. A gate driver malfunction occurs when the gate drive signal to the switch is interrupted. Thus, there is no signal to switch, creating an open-circuit fault in the IGBT switch A gate driver malfunction leads to an interruption in the gate drive signal to the switch, resulting in an open-circuit fault in the IGBT switch. This fault can arise from a faulty gate driver or bond wire lift-off within the IGBT switch. In cases where the anti-parallel diode is not integrated directly with the IGBT switch, it remains connected and operational [5], [9], [10]. An open-diode fault occurs when the diode is damaged and becomes disconnected from the circuit. In contrast, an open-switch fault occurs when both the IGBT and the diode within the circuit are faulty [5], [10], [11]. Such faults can manifest during bond wire lift-off caused by thermal stress, specifically in a Reverse Conducting Insulated Gate Bipolar Transistor (RC-IGBT) where the IGBT and diode are integrated on a single chip.

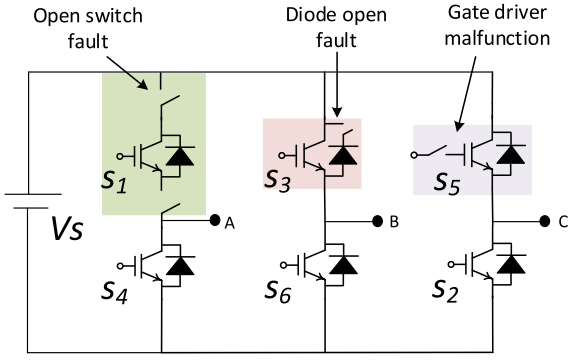

FIGURE 2. Possible open circuit faults in VSI.

Most studies on open-circuit faults have focused on gate drive malfunctions rather than on open-switch faults.

II. OPEN CIRCUIT FAULT DIAGNOSIS METHODS

Open circuit (OC) fault diagnosis can be categorized into model-based, data-driven, and signal-based approaches [1]. A model-based approach compares the information from the analytical and theoretical inverter models with that of a real system after a fault occurs. This includes the development of mathematical models and open- and closed-loop observers and using residuals as fault indicators. The authors of [12] used a switching-state function model for fault diagnosis in inverters. A gate-drive malfunction was created, the switching states were analyzed, and an estimated phase voltage was established. A normal scenario occurred when the measured and estimated phase voltages were similar. A threshold was set to consider measurement error, switching delay, and dead time. When a fault occurs, the phase voltage exceeds a set threshold. Thus, fault identification was achieved. However, only single-switch faults were identified in the present study. In [13], a Luenberger observer model was introduced using a *dq* stator current. The fault was identified by monitoring the current residuals and comparing them with a threshold value. Reference [4]presents an approach that uses an observer and an adaptive threshold to analyze system signals without extra hardware. It takes into account current dynamics, state changes, and real-world application factors. Its detection time is about 6ms. Reference [14] proposes a hybrid approach for diagnosing faults in sensorless induction motor drives. The method uses a diagnostic algorithm, based on a first-order sliding mode observer, to identify single and multiple open-switch faults and open-phase faults by analyzing unique features of the motor's abc frame in about 20% of the fundamental frequency. One of its drawbacks is the threshold setting. The main drawbacks of model-based approaches include a lack of robustness in multiple-switch fault identification and their dependence on the type of model used. Some voltage-based methods involve the use of extra equipment such as voltage sensors, thus reducing the total reliability and increasing the implementation cost.

A data-driven fault-diagnosis approach involves the use of machine learning for fault identification and localization. In this approach, significant emphasis is placed on the feature extraction of fault indicator signals, because they play a critical role in the performance of the technique. The raw three-phase current itself was combined with a random vector functional network in [15] for the fault identification and classification of gate-drive malfunction open-circuit faults. High accuracy can be achieved only when the sample's current time window length is greater than 60 ms (approximately 3-4 cycles). Wavelet analysis using a fuzzy algorithm was proposed in [15] and [16]. In this method, an open-circuit fault was created by opening the gate signal to the switches under investigation. The fault is detected by changes that occur in three-phase current wavelet coefficients. These coefficients were fed into the fuzzy algorithm for the fault identification and classification stages. Single- and double-switch faults were identified using this technique [16]. Several

combinations of wavelet parameters, such as wavelet energy and entropy, have been used with more sophisticated machine learning algorithms for fault identification [18], [19], [20]. The major concerns of the data-driven approach are its complexity and the requirement of large-scale data for training and validating machine-learning algorithms. Signal-based methods use the signal characteristics of current, voltage, or a combination of both for fault identification and classification. The following include different signal-based fault diagnosis techniques [16], [20], [21], which developed an open-circuit fault diagnosis (OC-FD) method based on the principle of the park vector technique by analyzing the average current trajectory. In a healthy condition, the average current trajectory is a complete circle; however, it is subject to change when a fault occurs. The shape of the current trajectory depends on the type of OC fault. The major drawback of this technique is its load dependence. To address this issue, the authors of [23] introduced a DC-normalized current that compares the normalized DC for each phase to a universal threshold. A pattern-recognition method was used in [23], that deploys three-phase current harmonics for FD was used in [23]. It has been established that whenever a fault occurs, the zero-order harmonics of the faulty phase are the sum of the other two zero-order harmonics of healthy phases. The faulty arm and single-switch faults can be identified; however, double-switch faults cannot be identified from the two different phases. Reference [25] introduces a novel fuzzy-based fault diagnosis technique for three-phase voltage-source inverters. It uses the average current Park's vector for detecting and locating single, multiple, and intermittent faults in power switches. These faults were detected in 9ms and the fuzzy system had an accuracy of 96%.

The mean current was proposed in [26] for fault identification and localization. Under normal conditions, the mean value of each phase is zero. However, this value changes when an OC fault exists. The polarity of the mean value was used for switch identification. Single- and double-switch faults can be identified; however, the technique is load dependent as well. To eliminate load dependency, an additional variable called the normalized mean current was employed [27]. This was derived by dividing the mean current of each phase by the Park modulus [26]. Under healthy conditions, the normalized average mean was 0.5198. Thus, a fault will cause deviation from the normalized healthy value. This technique can be used to identify single- and double-switch faults. A criticism of this method was published in [11], which indicated that this technique would not be effective at low currents, that is when the current approached zero. However, this technique cannot be used to identify triple-switch faults. Root-mean-square (RMS) and mean combination were proposed in [6] and [22]. It uses the RMS to identify the faulty arm and the mean to identify the faulty switch. It also introduces a normalized mean current to remove the load dependency. This technique cannot detect multiple switch faults and is prone to challenges that affect the normalization techniques discussed in other approaches.

The authors of [10] developed an FD method to identify open-switch faults in voltage-source inverters. This method is based on measuring the RMS and average voltage output of the inverter. It can identify single- and multiple-switch faults within a single cycle. The major drawback of this technique is the first step in the diagnosis, and it is necessary to compare the measured RMS voltage to the rated RMS voltage. Therefore, this technique requires the input of the rated RMS voltage at the start of FD.

Overall, the signal-based approach is simple and easy to implement in control units because minimum calculation is required [1]. Recent research has focused on a signal - and data-driven methods, owing to their simplicity and potential. The literature has shown that adding extra hardware, complexity, high cost of implementation, false alarms, and lack of robustness are major shortcomings of existing FD methods for OC faults.

Several authors such as [5], [10], and [11] have highlighted the potential for open switch faults to occur in inverter systems. Upon reviewing the literature, it's evident that much of the existing research predominantly concentrates on gate-drive malfunctions, with relatively fewer studies dedicated to open-switch faults in the inverter. Thus, distinguishing and accurately pinpointing the root causes of open-circuit faults in the inverter switches becomes an essential endeavour.

This paper's contributions are summarized as follows.

- A fault diagnosis technique for open-switch faults was developed using a combination of three-phase current average and rms for fault identification and classification.
- The FD technique can identify single and multiple switch faults without the need for additional sensors.
- It also introduces a novel but simple normalization technique to eliminate the load dependency associated with the mean current indicator compared with published methods.
- Developed a machine-learning-based technique that successfully identified single- and multiple-switch open-circuit faults. This was achieved by using supervised and ensemble-bagged tree models to predict the classification of faults that were completely independent of load changes.

The proposed model is verified experimentally to confirm the simulations.

In this paper, we present a comprehensive study of open-circuit fault diagnosis methods in Section II. In Section III, we discuss the specific characteristics of faults in the three-phase inverter output current. In Sections IV and V, we propose a novel fault-diagnosis method that utilizes average and RMS ratios. We then provide the simulation and experimental results in Sections VI and VII, respectively, before concluding our findings in Section VIII.

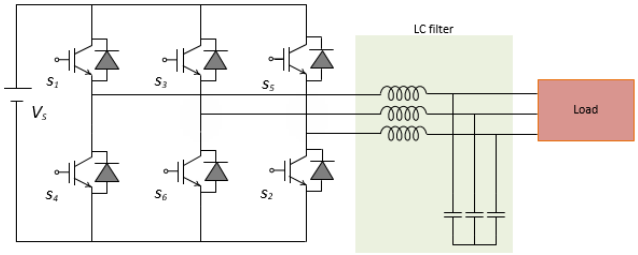

FIGURE 3. Three-phase inverter schematics.

III. OPEN CIRCUIT CHARACTERISTICS OF THREE-PHASE INVERTER

A. INVERTER MODEL

This study concentrates on a three-phase, two-level inverter system, as depicted in Fig. 3. The system utilizes IGBT switches and operates using pulse-width modulation (PWM) for control within an open-loop control framework. The output of this system is connected to an RL load, which is typically found in applications such as Uninterruptible Power Supplies (UPS), certain types of motor drives, renewable energy systems like solar photovoltaic and wind energy systems, and power supplies for electronic equipment. The specific parameters of the RL load, crucial for determining the performance of the system, are detailed in Table 1.

TABLE 1. Model parameters.

Parameters	Values
DC supply	100 V
Fundamental frequency	50 Hz
Carrier frequency	10 kHz
Load 1	4.7Ω, 5e-3 H
Load 2	10Ω, 10e-3 H
Load 3	3Ω, 10e-3 H
Modulation index	0.8
LC Filter	C= 25e-6, L =4.05e-3

B. FAULT ANALYSIS

The three-phase balanced output-current waveforms of the inverter are sinusoidal under normal operating conditions, as shown in Fig.4. This changes when an OC fault occurs in a single switch or multiple switches.

1) SINGLE SWITCH FAULT

When a switch from the upper arms is subjected to an OC fault (e.g., S3), the current will not flow through S3 but will flow through S6. Thus, the current in Phase B was negative. This, in turn, adds positive DC components to the currents in Phases A and C. The three-phase current became distorted, as shown in Fig. 5. The Case is reversed when S6 is OC and the current in phase B becomes positive.

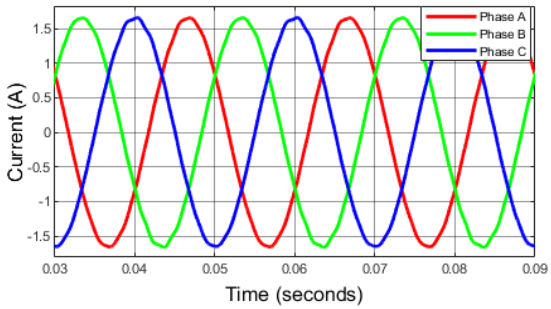

FIGURE 4. Three-phase current during healthy conditions.

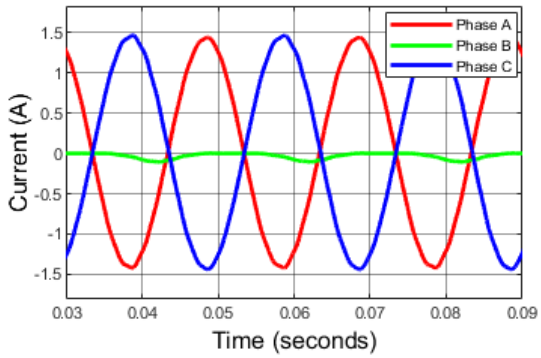

FIGURE 5. Open circuit fault on a single switch (S3).

2) DOUBLE SWITCH FAULT

During a double-switch OC fault on the upper arms (e.g., S1 and S3), the current does not flow through either Switch. Thus, the currents in phases A and B are negative, as shown in Fig. 6. The case is reversed if both the faulty switches are in the lower arms. The current waveform in the fault phase was positive. However, if one fault is in the upper arm and the other in the lower arm (e.g., S1 and S6), the current will not flow through them, thus creating positive and negative currents for phases A and B, respectively, as shown in Fig. 7.

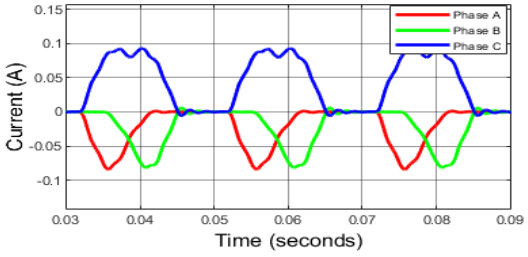

FIGURE 6. Open circuit faults on upper double switches (S1&S3).

3) TRIPLE SWITCH FAULT

When this type of fault occurs, all three-phase current waveforms have a positive or negative half cycle. This depends on the arm in which the fault occurred. If S4, S5, and S6 are affected by an OC fault, it can be observed in Fig.8 that

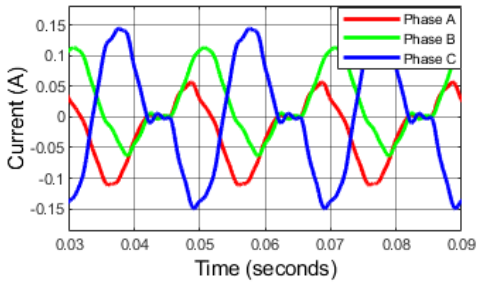

FIGURE 7. Open circuit faults on lower and upper switches (S1&S6).

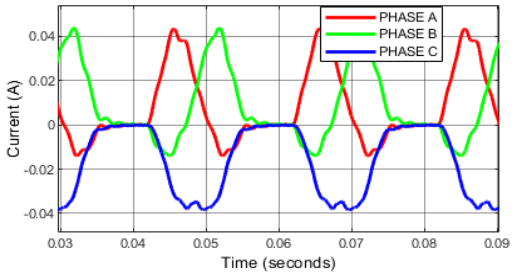

FIGURE 8. Open circuit faults on triple switches.

phases A and B will be positive, whereas phase C will have a negative value.

From this analysis, information from the current waveform can be extracted and used for fault identification during the OC faults.

IV. FAULT INDICATING MEASUREMENTS

In the previous section, it was established that the three-phase waveforms of the current are affected under faulty conditions. Thus, the waveform characteristics can be used as key indicators for identifying fault signatures. This study suggests using RMS and average values of the current for fault identification and classification. For example, Fig.9 shows the effect of the S1 OC fault on the average current. As can be observed, the average current is 0 during a healthy condition, and this changes during the fault when introduced at 0.04s. Fig.10 shows the effect of the S1 OC fault on the rms measured current. It is observed that during a healthy condition, the rms of all phases are the same but change when a fault is introduced at 0.04s. From all graphs, it is noticeable that the magnitude and sign of the average and rms currents are rich indicators of the type and location of faults.

V. NOVEL APPROACH OF FAULT DETECTION AND CLASSIFICATION

To extract information regarding the inverter condition, the RMS and average current values were calculated for each phase over one cycle using Eqs. (1) and (2), respectively: The RMS and average current values were generated from the simulated inverter for both healthy and faulty conditions to extract fault signatures. There are limitations to using each parameter individually for fault detection. The RMS

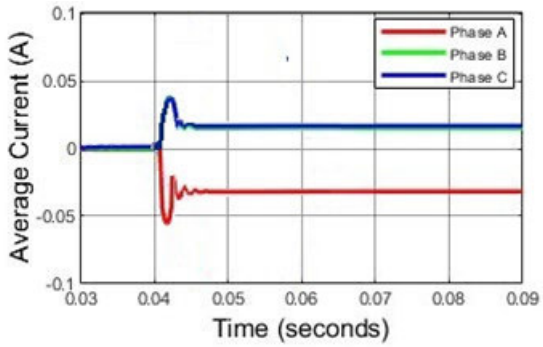

FIGURE 9. Three-phase average current during S1 OC fault.

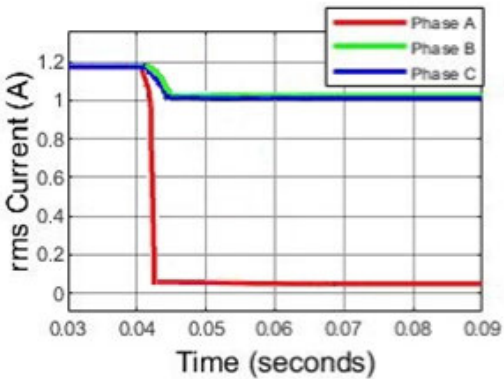

FIGURE 10. Three-phase rms current during S1 OC fault.

alone can identify the faulty phase in the inverter, but cannot identify the faulty switch. This is also load dependent.

$$I_{avg} = \frac{1}{T}\int_0^T i\,(t)dt \tag{1}$$

$$I_{rms} = \sqrt{\frac{1}{T}\int_0^T i^2\,(t)dt} \tag{2}$$

Using only the average current, identification of the faulty switch and/or phase (only if one or two phases are faulty) can be achieved; however, the FD method is load dependent and cannot differentiate between short- and open-circuit faults. To address the load dependency issue, researchers have adopted an additional variable called the normalized mean current [27]. This was derived by dividing the mean current of each phase by the Park modulus [26]. However, this normalization technique has limitations, including lower effectiveness at low current values and the inability to identify triple-switch faults [1].

This study presents a new normalization technique that uses the ratio of the average to the RMS current for each phase. The average and RMS values changed at different loads, but the average-to-RMS ratio remained the same. Table 2 shows a sample of the average-rms ratio for the S3 fault for different loads, as indicated in Fig.11.

Thus, the mean to rms ratio can be employed for fault detection without being load dependent. This technique has

TABLE 2. AVERAGE/RMS ratio oc single switch s3 fault.

Phase	Loads	rms-B	average-B	average/rms ratio
A	Load 1	1	0.016	0.016
	Load 2	0.51	0.0081	0.016
	Load 3	1.03	0.0165	0.016
B	Load 1	0.049	-0.0323	-0.66
	Load 2	0.046	-0.030	-0.66
	Load 3	0.049	-0.0323	-0.66
C	Load 1	1	0.016	0.016
	Load 2	0.52	0.0083	0.016
	Load 3	1.06	0.0169	0.016

TABLE 3. Sample of average to rms ratio value for different loads during O.C single and multiple switch faults.

Faulty switch	A	B	C	A	B	C
Load	Load 1			Load 2		
Healthy	0	0	0	0	0	0
S1 OC	-0.66	0.016	0.016	-0.66	0.016	0.016
S3 OC	0.01	-0.66	0.016	0.01	-0.66	0.016
S3S5 OC	0.76	-0.62	-0.62	0.76	-0.62	-0.62
S1S5 OC	-0.62	0.76	-0.62	-0.62	0.76	-0.62
S1S2S3 OC	-0.43	-0.44	0.7	-0.43	-0.44	0.7
S4S5S6 OC	0.43	0.44	-0.7	0.43	0.44	-0.7

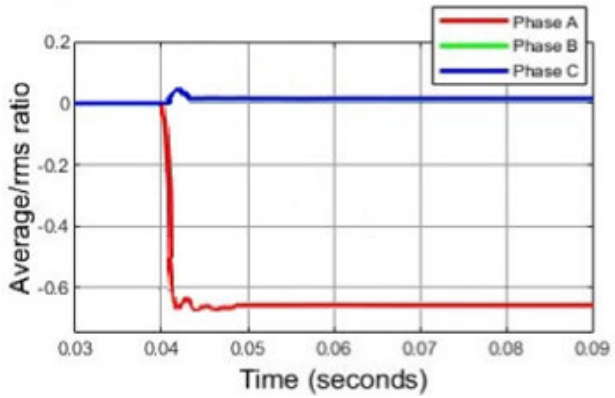

FIGURE 11. Average / rms ratio OC single switchS1 fault.

been shown to identify faults at low currents and triple-switch faults in the inverters. The sample data given in Table 3 represent the generated data to be presented to a machine-learning algorithm to classify the faulty switch of the faulty phase (A/B/C) under load variation. Table 4 lists all the possible open-switch faults and their respective fault labels. These fault labels are used to train the classifiers.

A. CLASSIFICATION TECHNIQUES

Several classifiers are used in the decision-making process for fault identification in the inverters. Accuracy and efficiency are critical factors when considering the best classifiers. Support vector machine (SVM), Naïve Bayes (NB) (KNN) decision tree (DT), and linear discriminant are some of

TABLE 4. Fault type labels.

Fault type	Fault label	Fault type	Fault label
Healthy	0	S1S6 OC	13
S1 OC	1	S3S4 OC	14
S3 OC	2	S1S2 OC	15
S5 OC	3	S4S5 OC	16
S4 OC	4	S2S3 OC	17
S6 OC	5	S5S6 OC	18
S2 OC	6	S1S2S3 OC	19
S3S5 OC	7	S4S5S6 OC	20
S1S5 OC	8	S1S5S6 OC	21
S1S3 OC	9	S2S3S4 OC	22
S2S6 OC	10	S1S2S6 OC	23
S2S4 OC	11	S3S4S5 OC	24
S4S6 OC	12		

the classifiers used in fault classification. The accuracy of these classifiers significantly depends on the dataset parameters; thus, the accuracy varies from one dataset to another. To achieve a high classifier model efficiency, cross-validation was applied to the training process to protect against overfitting. This was achieved by segmenting the dataset into smaller sets and estimating their accuracy.

1) SUPPORT VECTOR MACHINE

This supervised machine-learning technique was developed in [30] and used for both classification and regression analyses. This technique is based on determining the optimal separating hyperplane between two classes of data, as illustrated in Fig.12 [31]. A hyperplane with the maximum distance between the two data classes was chosen. Its major advantage is its ability to produce a globally optimized separating boundary using a small dataset compared with a neural network that uses a large dataset and has a high risk of local minima [20].

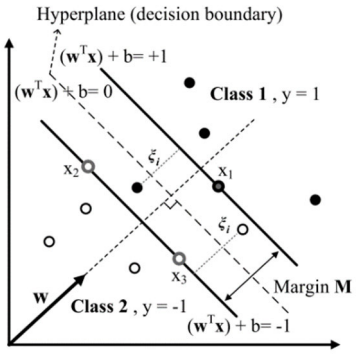

FIGURE 12. SVM classifier [31].

Maximize

$$W(\alpha) = \sum_{j=1}^{N} \alpha_i - \frac{1}{2} \sum_{i=1}^{N} \sum_{j=1}^{N} \alpha_i \alpha_j y_i y_j K\left(\mathbf{x}_i, \mathbf{x}_j\right) \quad (3)$$

Subjected to

$$\sum_{i=1}^{N} \alpha_i y_i = 0, \quad 0 \le \alpha_i \le C, \quad \forall i = (1, 2, \ldots, N) \quad (4)$$

$$K\left(\mathbf{x}, \mathbf{x}'\right) = \left(< \mathbf{x}, \mathbf{x}' > +1\right)^d \quad (5)$$

where α_i is a Lagrange multiplier, and $(\mathbf{x}_i, y_i)$ is a training dataset in which $\mathbf{x}_i$ is the input data and y_i is the output data. C is a constant for a trade-off between the performance and the generalization, $K(\mathbf{x}, \mathbf{x}')$ is a polynomial kernel function that performs the non-linear mapping into the feature space.

2) K- NEAREST NEIGHBOURS

It is one of the simplest forms of supervised machine learning that can be used for classification and regression. Classification is conducted by mapping how close data classes are and grouping them based on their minimum distances as nearest neighbours [20], [32]. Fig.13 shows the general KNN classifier. In this scenario, the Euclidean KNN model was adopted using Equation (6) [33], which measures the straight-line distance between classes of x_1 and x_2.

$$d\left(x_1, x_2\right) = \sqrt{\sum_{j=1}^{p} \left(x_1 - x_2\right)^2} \quad (6)$$

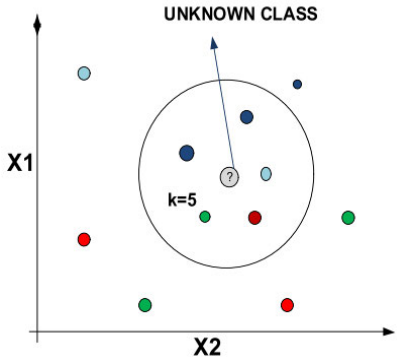

FIGURE 13. KNN classifier [20].

3) DECISION TREE

This method graphically represents the steps that must be performed to achieve optimal classification. It is a supervised machine learning method that solves problems using a top-bottom approach to find solutions [20], [34]. All possibilities were considered before making the final decision.

4) ENSEMBLE DECISION TREE

Ensemble learning is a supervised machine learning method with a high ability to accurately predict classification labels [35]. This is a series/parallel combination of classifiers to improve the classification accuracy, generalizability, and robustness over a single classifier.

Several ensemble methods have been proposed to achieve this purpose. This paper uses the bagging tree method. A bagging tree is a combination of decision tree classifiers, which results in a reduction in the variance and bias of the classifiers, thus improving accuracy. Fig. 14 shows the basic structure of the bagging decision tree. This study used 30 learners in the bagged tree method to enhance the classifier output.

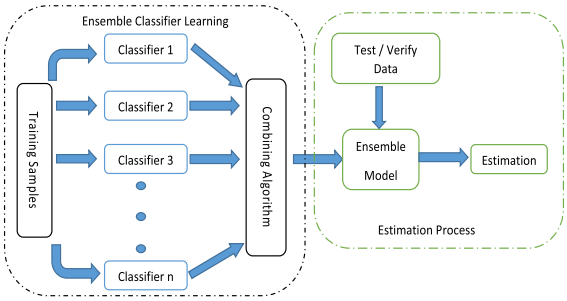

FIGURE 14. Bagging structure.

B. PROPOSED CLASSIFICATION ASSESSMENT

Single- and multiple-switch OC faults were simulated using MATLAB and Simulink. Table 3 shows a sample of the average, RMS, and their ratio values for different loads during the OC single and multiple switch faults. These values are then used to train the classifier models. To achieve high accuracy in identifying fault conditions, several techniques were compared for the same set of supervised training data. Classifiers based on trees, KNN, SVC, and ensembles were trained and their responses were studied. An indicator called the Confusion Matrix was used to evaluate the performance of each classifier in retrieving the original trained state.

The confusion matrix plots show the performance of the classifier for each class of the dataset. The true class was plotted against the predicted class. Thus, the diagonal class indicates classifier performance. The confusion matrix is analyzed based on two factors namely the false discovery rates (FDR), and predictive Positive values (PPV). FDR is defined as the proportion of erroneously categorized observations per expected class, whereas PPV is defined as the proportion of correctly categorized observations per projected class. In the confusion matrix, the highest FDR is denoted in red and the highest PPV is denoted in green. As the FDR and PPV values decreased, the intensity of the colour decreased. It is important to note that when the PPV is not at its highest, there is a presence of FDR

Fig. 15 shows the confusion matrix for the decision tree classifier when trained with the average and rms ratios. From the figure, we can observe that there are many FDR and most PPVs do not reach 100%. This indicates that the classifier cannot accurately distinguish the fault classes. An example with the S5 open switch fault is denoted as fault label '3' on the confusion matrix. The PPV was 53% and the accumulated FDR was approximately 46.7%. This means that the classifier tends to classify S5 faults as other faults. In this case, S2S3, S4S6, and S4S5S6 faults are denoted by their corresponding fault labels 12, 17, and 20, respectively.

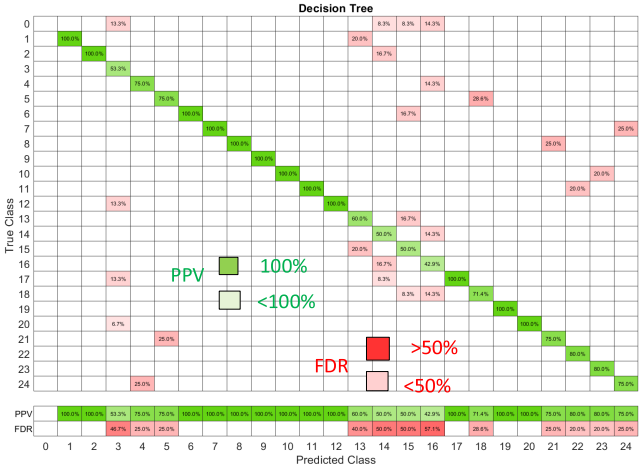

FIGURE 15. Decision tree confusion matrix.

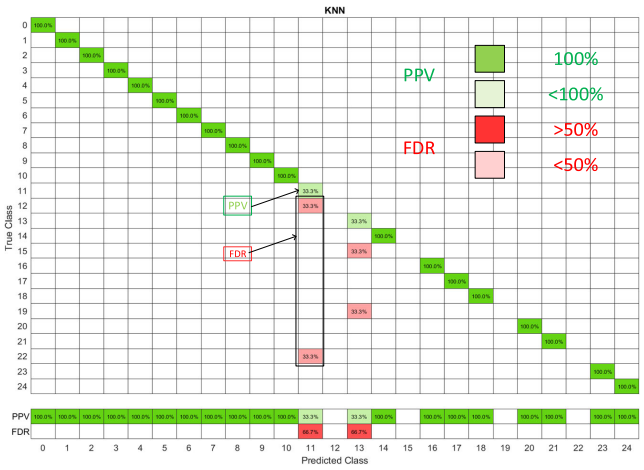

FIGURE 16. KNN confusion matrix.

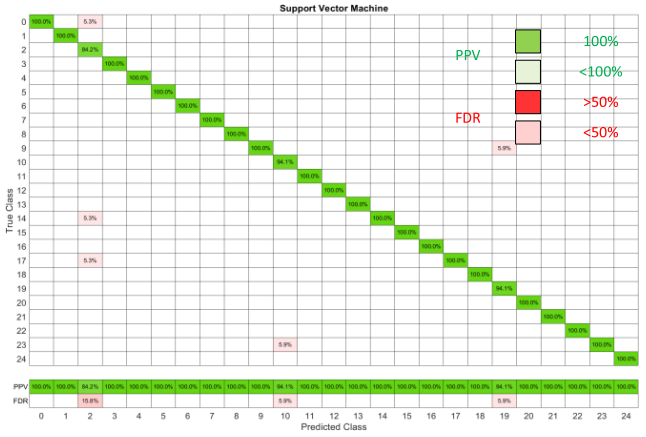

FIGURE 17. SVM confusion matrix.

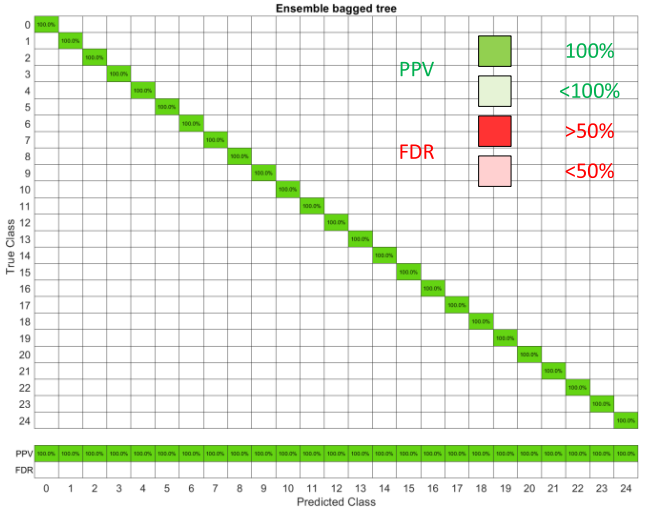

FIGURE 18. Ensemble bagged tree confusion matrix.

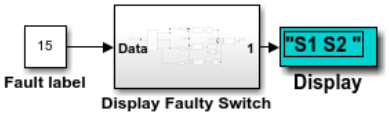

FIGURE 19. Fault label to display conversion.

Fig.16 and 17 show the confusion matrices of KNN and SVM, respectively. Both can be observed to have an FDR; therefore, they can incorrectly classify trained open-switch faults. However, in the SVM confusion matrix, it can be observed that FDR has a lower colour intensity than KNN and the decision tree. This indicates that SVM performs better than KNN and the decision tree.

Fig.18 shows the confusion matrix for the ensemble-bagged tree. It can be observed that the classifier did not misclassify the different faults; hence, the PPV for each fault was 100%. From the confusion matrices for the different classifiers, it is clear that the bagged ensemble has the highest accuracy in estimating classes that are as close as possible to the true values.

VI. SIMULATION RESULTS

A three-phase DC-AC inverter was simulated under different fault scenarios for IGBT open-circuit faults. The test model included the inverter under investigation, with an ensemble classifier block fed from the current RMS and average measurements. The machine learning block (classification model) has three main functions: first, to check and identify the healthy case from the faulty phase; second function) to apply ensemble classifications for the average/rms data samples, and (third) to convert the fault label values to string output showing the faulty switch on the display. The numeric-to-string conversion is implemented using a mathematical function in MATLAB. A schematic of the process is shown in Fig. 19. The fault label values were split into single digits and converted into strings. This signal was then fed into the display to show the condition of the inverter. This creates a user-friendly environment for the proposed method.

A flowchart of the classification system is shown in Fig. 20. The output of the classifier is indicated as a "figure" that represents the fault case, and the full details of all cases are given in Table 4 for all possible fault open circuits, that is, for single, double, and triple faulty switches (es).

TABLE 5. Classifier performance.

Classifier	Average training time	Average testing accuracy
Support vector machine	7.05s	98.7%
K- Nearest Neighbours	1.50s	89.3%
Decision Tree	1.02s	77.0%
Ensemble decision tree	1.05s	100%

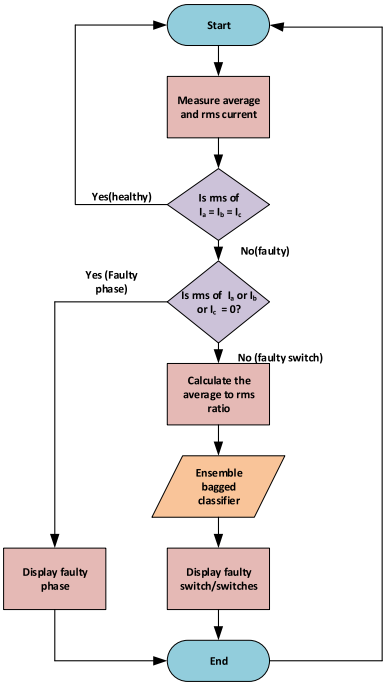

FIGURE 20. Fault diagnosis flow chart.

The simulation analysis and the results of the investigated technique are presented in this section. Table 5 shows that the ensemble bagged classifier has the best performance and accuracy (100%) compared to the other classifiers.

Fig. 21 – 24 shows the simulation fault diagnosis model results for OC single-, double-, and triple-switch faults, respectively, using the ensemble-bagged supervised classification technique. The display faulty switch block is designed to convert the classifier fault indicator into a display of fault type and indicates the faulty switch(es).

As shown in Fig. 21, S3 was an open-circuit circuit. The corresponding average to-RMS ratios are shown in Fig. 10. The output fault label code of that fault according to Table 4 is 2, this is also indicated in the display unit as 'S3' which is clearly shown.

Fig. 22 shows the classifier outputting 'S1 S3' for the double open-circuit switches in the top arms, in this case, for S1 and S3. The resulting output shows the fault label as '9' as indicated in Table 4.

Fig. 23 shows the classifier result when two switches from two different phases are open-circuited, this is S2&S3, it produces the code of '17' as indicated in Table 4

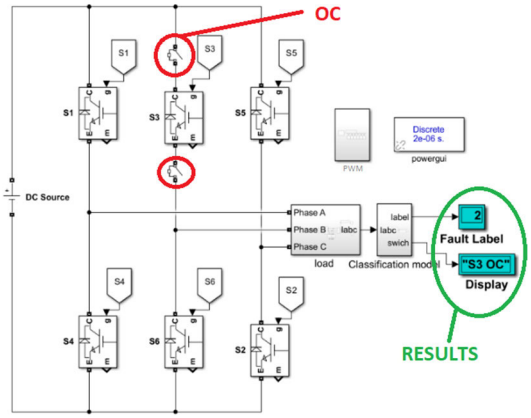

FIGURE 21. Simulation fault diagnosis result for S3 OC.

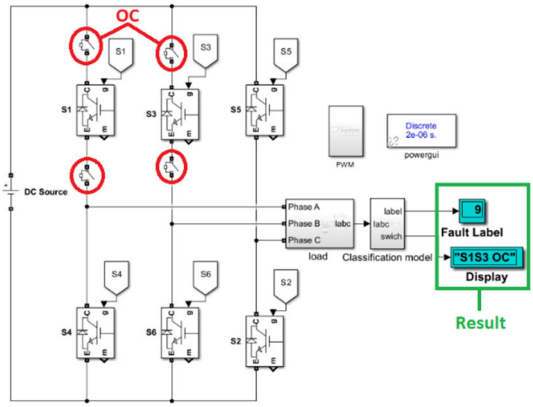

FIGURE 22. Simulation fault diagnosis result for S1S3 OC.

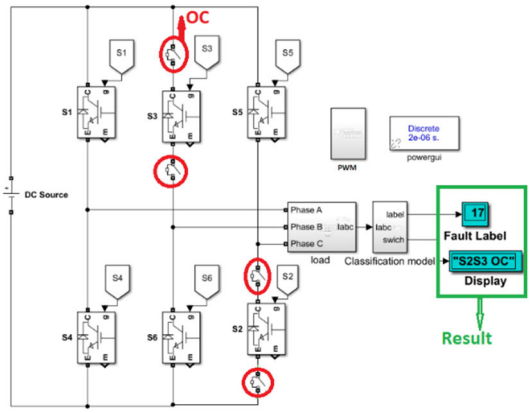

FIGURE 23. Simulation fault diagnosis result for S2S3 OC.

Fig.24 shows the classifier estimation for triple switches open circuit fault for S1&S2&S3, it produces the correct fault code of '19.'

Fig. 25 shows the different fault scenarios and fault diagnosis technique responses to these faults. From Fig. 25A a healthy scenario is simulated from 0 – 0.11 s and it can be seen that the current waveform is sinusoidal thus the fault technique reads '0' indicating a normal condition. An open

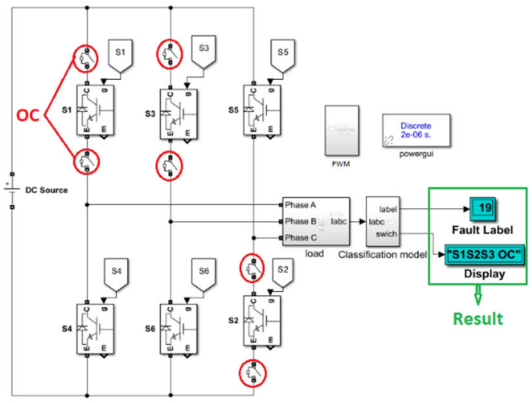

FIGURE 24. Simulation fault diagnosis result for S1S2S3 OC.

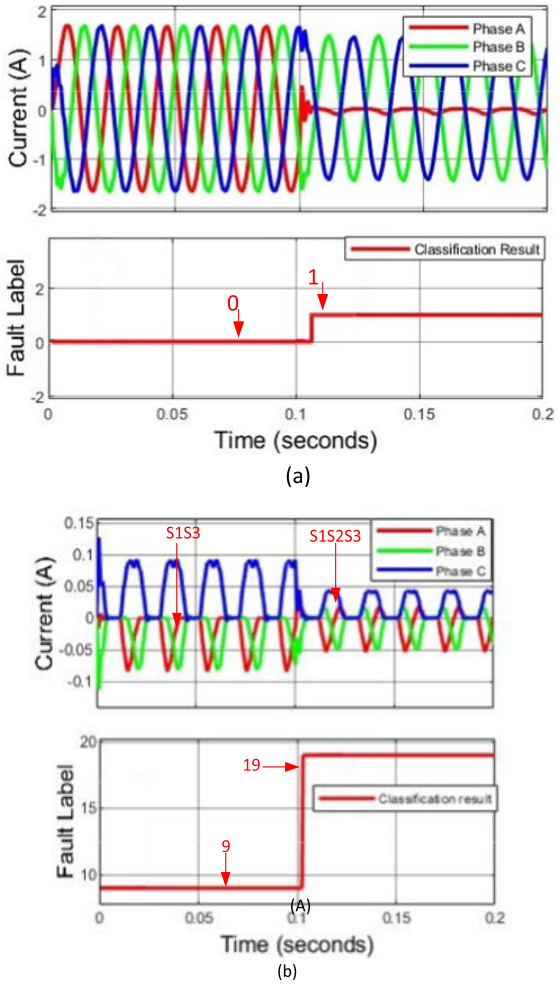

FIGURE 25. Fault diagnosis response to different open switch faults (a) Diagnosis response to S1 fault (b) Diagnosis response to S1S3 and S1S2S3 Open switch fault.

switch fault S1 is introduced between 0.11 s – 0.2 s. Phase A will have negative values and the fault diagnosis technique result changes from '0' to '1' according to the fault label in Table 4. Fig. 25B shows a double-switch open circuit S1, and

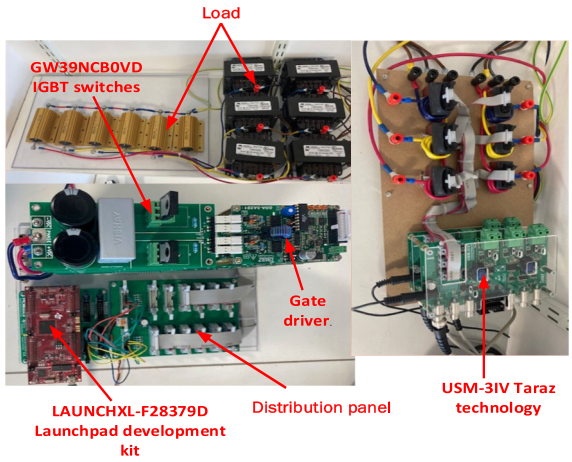

FIGURE 26. Experiment setup.

S3 is introduced from 0 to 0.1s. The fault diagnosis technique immediately identifies faulty switches by indicating fault label '9 ' at a diagnosis time of 12.5% of the fundamental frequency approximately 2.5ms. A triple switch open circuit fault S1, S2 and S3 is introduced at 0.1s -0.2s, and we can observe the decrease in the magnitude of the current waveform thus the fault diagnosis technique indicates '19. ' These results demonstrate that the proposed technique can identify the fault switch for half the period of the fundamental frequency.

VII. EXPERIMENT RESULT

The experimental setup was performed at the Smart Energy Lab at the Glasgow Caledonian University, as shown in Fig. 26. The setup included a three-phase inverter with six removable GW39NCB0VD IGBT switches driven by a GDA-3A2S1 Taraz Technologies gate driver. MATLAB Simulink was used to generate the gate control signals for the six switches. The LAUNCHXL-F28379D Launchpad Development Kit was used as an input–output interface between the Simulink and gate drivers. An open-circuit fault was created by removing each switch, and the three-phase output current was measured using a current and voltage measurement device USM-31V (Taraz Technologies). The data from the phase current measurements were logged from the oscilloscope and fed offline to the fault diagnosis model block in MATLAB Simulink and were used for fault identification and classification.

Fig. 27-28 shows the output currents for the healthy and faulty case obtained from the experiment.

Fig. 29 shows the Simulink fault diagnosis model fed with the experimental three-phase current. In this case, a single (S3) open switch fault is fed to the model and the output of the model indicates S3 while the fault label shows '2'. In Fig. 30, a more detailed diagram can be observed when the S3 open-switch fault was applied, and the fault diagnosis model increased to 2. This indicates that the faulty switch is S3.

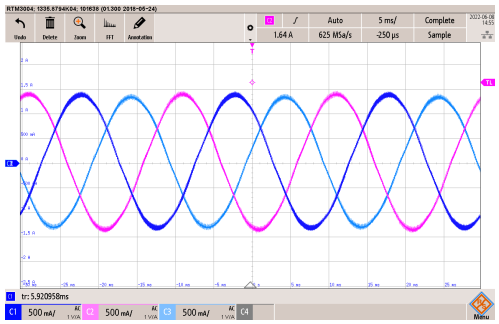

FIGURE 27. Experimental three-phase current for a healthy condition.

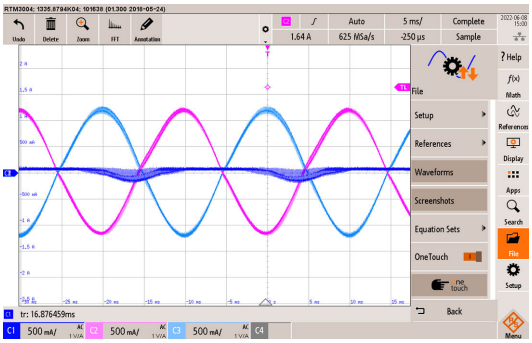

FIGURE 28. Experimental three-phase current for S3 OC fault.

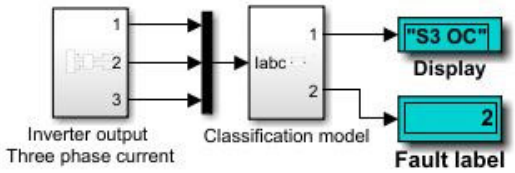

FIGURE 29. Simulink experiment result for S3 OC fault.

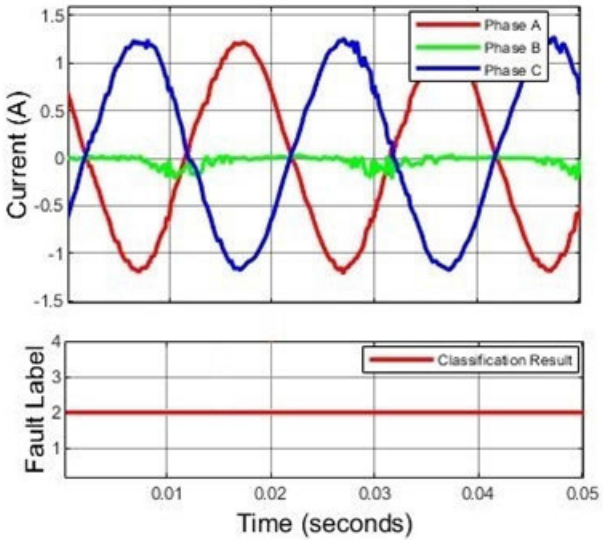

FIGURE 30. Fault diagnosis experimental result for S3 OC fault.

The experimental results verified the proposed technique in all scenarios, and all single- and multiple-switch OC faults could be detected and classified accurately.

TABLE 6. Comparative result.

Fault diagnosis technique	Diagnosis parameter	Diagnosis time (ms)	Accuracy (%)
An Average Model-Based Transistor Open-Circuit Fault Diagnosis Method for Grid-Tied Single-Phase Inverter [36]	Voltage signals	5.8	-
fault diagnosis of inverters based on current trajectory [37]	Three phase Phase	10	-
Current covariance analysis-based open-circuit fault diagnosis [3]	covariance of three-phase current	8	-
Observer-based adaptive threshold diagnosis method for open-switch [4] faults of voltage source inverters	System model	6	-
wavelet transform and support vector machine [38]	Wavelet coefficient of the three-phase current	7	84.54
Using CEEMDAN algorithm and SVM Fault Diagnosis [39]	Clarke transform of the three-phase current	3.8	95.45
Fuzzy Control Based Double Switching Fault Tolerant Control on Four Switch Voltage Source Inverters [40]	System model	10	98
PWM-VSI Fault Diagnosis for a PMSM Drive Based on the Fuzzy Logic Approach [25]	Phase current	9	96
Open-Switch Fault Diagnosis Method in Voltage-Source Inverters Based on Phase Currents [26]	Three phase current	4	-
Improved diagnosis method for VSI-fed IM drives under open IGBT faults [6]	System model	6	-
Proposed method	Current RMS and Average ratio	2.5	100

Table 6 presents a comparative analysis of the proposed fault diagnosis technique, specifically for IGBT/Diode faults, against techniques previously used for IGBT faults, with a particular emphasis on detection time and accuracy. The detection time is evaluated in relation to the period of the fundamental current, which is 20ms. The data in Table 6 clearly shows that most of the techniques require less than half the period of the fundamental time for diagnosis. Moreover, the table illustrates that the proposed method for IGBT/Diode faults demonstrates strong performance across the evaluated parameters, indicating its effectiveness in a comparative context, rather than a direct comparison of the fault diagnosis methods themselves.

VIII. CONCLUSION

This study focused on the open-switch fault of a three-phase inverter. This study presents a new fault diagnosis method for identifying and classifying single and multiple open-switch faults. This was achieved by.

- The three-phase current waveform of the inverter was analyzed, and the average and RMS values were extracted. The combination of both parameters yields a robust fault diagnosis method compared with using them individually.
- A new normalization method based on the mean-to-RMS ratio is introduced and verified. The ratio values were fed into the ensemble-bagged classification method to classify different faults.

- The proposed technique can identify multiple switch faults including triple-switch faults. It is also effective under low current conditions.
- In addition to the simplicity of the fault diagnosis technique, additional sensors are not required, thus facilitating implementation and minimizing the cost to the manufacturer.
- The proposed fault diagnosis technique was validated through experiments and simulations. The results presented in this paper confirm the robustness of the proposed technique for estimating all possible fault scenarios.

REFERENCES

[1] K. Hu, Z. Liu, Y. Yang, F. Iannuzzo, and F. Blaabjerg, "Ensuring a reliable operation of two-level IGBT-based power converters: A review of monitoring and fault-tolerant approaches," *IEEE Access*, vol. 8, pp. 89988–90022, 2020.

[2] T. Chen, Y. Pan, and Z. Xiong, "Fault diagnosis scheme for single and simultaneous open-circuit faults of voltage-source inverters on the basis of fault online simulation," *J. Power Electron.*, vol. 21, no. 2, pp. 384–395, Feb. 2021.

[3] H. Yang, Y. Zhou, and J. Zhao, "Current covariance analysis-based open-circuit fault diagnosis for voltage-source-inverter-fed vector-controlled induction motor drives," *J. Power Electron.*, vol. 20, no. 2, pp. 492–500, Mar. 2020.

[4] H. Yin, Y. Chen, and Z. Chen, "Observer-based adaptive threshold diagnosis method for open-switch faults of voltage source inverters," *J. Power Electron.*, vol. 20, no. 6, pp. 1573–1582, Nov. 2020.

[5] S. M. Dabour and M. I. Masoud, "Open-circuit fault detection of five-phase voltage source inverters," in *Proc. IEEE 8th GCC Conf. Exhib.*, Feb. 2015, pp. 1–6.

[6] M. A. Zdiri, B. Bouzidi, and H. H. Abdallah, "Improved diagnosis method for VSI fed IM drives under open IGBT faults," in *Proc. 15th Int. Multi-Conf. Syst., Signals Devices (SSD)*, Mar. 2018, pp. 905–910.

[7] M. Hossain, A. Abu-Siada, and S. Muyeen, "Methods for advanced wind turbine condition monitoring and early diagnosis: A literature review," *Energies*, vol. 11, no. 5, p. 1309, May 2018.

[8] M. D. Kumar, S. F. Kodad, and B. Sarvesh, "Simplified fault detection algorithm for voltage source fed induction motor," *Mater. Today, Proc.*, vol. 5, no. 1, pp. 1401–1410, 2018.

[9] Z. Li, H. Ma, Z. Bai, Y. Wang, and B. Wang, "Fast transistor open-circuit faults diagnosis in grid-tied three-phase VSIs based on average bridge arm pole-to-pole voltages and error-adaptive thresholds," *IEEE Trans. Power Electron.*, vol. 33, no. 9, pp. 8040–8051, Sep. 2018.

[10] Y. O. Ajra, H. A. Sheikh, N. Moubayed, and G. Hoblos, "Fault diagnosis of open switch failure in voltage source inverter using average and RMS phase voltages," in *Proc. Int. Conf. Innov. Intell. for Informat., Comput., Technol. (3ICT)*, Sep. 2021, pp. 250–255.

[11] L. M. Halabi, I. M. Alsofyani, and K.-B. Lee, "Open circuit fault diagnosis for multi-level inverters using an improved current distortion method," in *Proc. IEEE Conf. Energy Convers. (CENCON)*, Oct. 2021, pp. 75–79.

[12] T. Yanghong, Z. Haixia, and Z. Ye, "A simple-to-implement fault diagnosis method for open switch fault in wind system PMSG drives without threshold setting," *Energies*, vol. 11, no. 10, p. 2571, Sep. 2018.

[13] Y. Chen, H. Luo, W. Li, X. He, F. Iannuzzo, and F. Blaabjerg, "Analytical and experimental investigation on a dynamic thermo-sensitive electrical parameter with maximum dIC/dt during turn-off for high power trench gate/field-stop IGBT modules," *IEEE Trans. Power Electron.*, vol. 32, no. 8, pp. 6394–6404, Aug. 2017.

[14] R. Maamouri, M. Trabelsi, M. Boussak, and F. M'Sahli, "Mixed model-based and signal-based approach for open-switches fault diagnostic in sensorless speed vector controlled induction motor drive using sliding mode observer," *IET Power Electron.*, vol. 12, no. 5, pp. 1149–1159, May 2019.

[15] Y. Xia, B. Gou, Y. Xu, and G. Wilson, "Ensemble-based randomized classifier for data-driven fault diagnosis of IGBT in traction converters," in *Proc. IEEE Innov. Smart Grid Technol. Asia (ISGT Asia)*, May 2018, pp. 74–79.

[16] H. S. H. Chung, H. Wang, F. Blaabjerg, and M. Pecht, *Reliability of Power Electronic Converter Systems*. Institution of Engineering and Technology, 2016.

[17] S. Anupama and S. Priya, "Open circuit switch fault diagnosis methods for VSI fed induction motor drive," in *Proc. 3rd Int. Conf. Adv. Comput. Commun. Syst. (ICACCS)*, vol. 1, Jan. 2016, pp. 1–6.

[18] R. B. Dhumale and S. D. Lokhande, "Comparative study of fault diagnostic methods in voltage source inverter fed three phase induction motor drive," *IOP Conf. Ser., Mater. Sci. Eng.*, vol. 197, no. 1, 2017, Art. no. 012006.

[19] Z. Yang and Y. Chai, "A survey of fault diagnosis for onshore grid-connected converter in wind energy conversion systems," *Renew. Sustain. Energy Rev.*, vol. 66, pp. 345–359, Dec. 2016.

[20] P. Achintya and L. Kumar Sahu, "Open circuit switch fault detection in multilevel inverter topology using machine learning techniques," in *Proc. IEEE 9th Power India Int. Conf. (PIICON)*, Feb. 2020, pp. 1–6.

[21] A. M. S. Mendes and A. J. M. Cardoso, "Voltage source inverter fault diagnosis in variable speed AC drives, by the average current park's vector approach," in *Proc. IEEE Int. Electr. Mach. Drives Conf. (IEMDC)*, May 1999, pp. 704–706.

[22] B. Lu and S. K. Sharma, "A literature review of IGBT fault diagnostic and protection methods for power inverters," *IEEE Trans. Ind. Appl.*, vol. 45, no. 5, pp. 1770–1777, Sep./Oct. 2009.

[23] K. Rothenhagen and F. W. Fuchs, "Performance of diagnosis methods for IGBT open circuit faults in three phase voltage source inverters for AC variable speed drives," in *Proc. Eur. Conf. Power Electron. Appl.*, 2005, pp. 1–10.

[24] C. B. D. Eddine, B. Azzeddine, K. M. Amine, B. Mokhtar, and B. Noureddine, "The enhancement of park current vectors technique for inverter fault detection," in *Proc. 6th Int. Conf. Syst. Control (ICSC)*, May 2017, pp. 377–382.

[25] H. Yan, Y. Xu, F. Cai, H. Zhang, W. Zhao, and C. Gerada, "PWM-VSI fault diagnosis for a PMSM drive based on the fuzzy logic approach," *IEEE Trans. Power Electron.*, vol. 34, no. 1, pp. 759–768, Jan. 2019.

[26] Z. Jian-Jian, C. Yong, C. Zhang-Yong, and Z. Anjian, "Open-switch fault diagnosis method in voltage-source inverters based on phase currents," *IEEE Access*, vol. 7, pp. 63619–63625, 2019.

[27] J. O. Estima and A. J. Marques Cardoso, "A new approach for real-time multiple open-circuit fault diagnosis in voltage source inverters," in *Proc. IEEE Energy Convers. Congr. Expo.*, Sep. 2010, pp. 4328–4335.

[28] M. A. Khelif, A. Bendiabdellah, and B. D. E. Cherif, "A combined RMS-MEAN value approach for an inverter open-circuit fault detection," *Periodica Polytechnica Electr. Eng. Comput. Sci.*, vol. 63, no. 3, pp. 169–177, Apr. 2019.

[29] P. S. Das and K. H. Kim, "Open-switch fault-tolerant control of a grid-side converter in a wind power generation system," *Int. J. Power Electron. Drive Syst.*, vol. 6, no. 2, pp. 293–304, 2015.

[30] C. Cortes and V. Vapnik, "Support-vector networks," *Mach. Learn.*, vol. 20, no. 3, pp. 273–297, 1995.

[31] D.-E. Kim and D.-C. Lee, "Fault diagnosis of three-phase PWM inverters using wavelet and SVM," in *Proc. IEEE Int. Symp. Ind. Electron.*, vol. 2, Jun. 2008, pp. 329–334.

[32] W. Gong, H. Chen, Z. Zhang, M. Zhang, and H. Gao, "A data-driven-based fault diagnosis approach for electrical power DC–DC inverter by using modified convolutional neural network with global average pooling and 2-D feature image," *IEEE Access*, vol. 8, pp. 73677–73697, 2020.

[33] B. Boehmke and B. Greenwell, *Hands-On Machine Learning With R*. London, U.K.: Chapman & Hall, 2019.

[34] A. Stetco, F. Dinmohammadi, X. Zhao, V. Robu, D. Flynn, M. Barnes, J. Keane, and G. Nenadic, "Machine learning methods for wind turbine condition monitoring: A review," *Renew. Energy*, vol. 133, pp. 620–635, Apr. 2019.

[35] W. Zhu, M. Xie, and J.-F. Xie, "A decision tree algorithm for license plate recognition based on bagging," in *Proc. Int. Conf. Wavelet Act. Media Technol. Inf. Process. (ICWAMTIP)*, Dec. 2012, pp. 136–139.

[36] Z. Li, B. Wang, Y. Ren, J. Wang, Z. Bai, and H. Ma, "An average model-based transistor open-circuit fault diagnosis method for grid-tied single-phase inverter," in *Proc. 44th Annu. Conf. IEEE Ind. Electron. Soc. (IECON)*, Oct. 2018, pp. 993–998.

[37] K.-D. Li, C.-Y. Chen, T.-F. Chen, S. Cheng, X. Wu, and C.-Q. Xiang, "A new approach for on-line open-circuit fault diagnosis of inverters based on current trajectory," *J. Central South Univ.*, vol. 26, no. 3, pp. 743–758, Mar. 2019.

[38] M. Fei, L. Ning, M. Huiyu, P. Yi, S. Haoyuan, and Z. Jianyong, "On-line fault diagnosis model for locomotive traction inverter based on wavelet transform and support vector machine," *Microelectron. Rel.*, vols. 88–90, pp. 1274–1280, Sep. 2018.
[39] L. Qiu, Q. Peng, Y. Yang, W. Xu, and Q. Liang, "Using CEEMDAN algorithm and SVM fault diagnosis methodology in three-phase inverters of PMSM drive systems," in *Proc. 36th Chin. Control Conf. (CCC)*, Jul. 2017, pp. 7127–7132.
[40] M. Ayyakrishnan, "Fuzzy control based double switching fault tolerant control on four switch voltage source inverters," *J. Electr. Eng. Technol.*, vol. 17, no. 2, pp. 1031–1038, Mar. 2022.

CHUKWUEMEKA N. IBEM (Member, IEEE) received the B.Eng. degree (Hons.) in electrical electronics engineering from the Bells University of Technology, Nigeria, in 2015, and the M.Sc. degree in electrical electronics engineering from Glasgow Caledonian University, U.K., in 2017, where he is currently pursuing the Ph.D. degree. The Ph.D. topic is based on developing robust fault detection techniques and tolerant schemes for converter topologies. He has published conference papers in the IEEE. His current research interests include fault analysis of converter topologies, renewable energy topology integration, renewable energy storage, and distributed generation systems.

MOHAMED E. FARRAG (Member, IEEE) received the B.Eng. (Hons.) and M.Sc. degrees in industrial electronics and control engineering from Egypt, in 1990 and 1996, respectively, and the Ph.D. degree from Northumbria University, U.K., in 2002. He is currently a Professor with the Department of Electrical and Electronic Engineering, Glasgow Caledonian University (GCU), U.K., with more than 20 years of research and lecturing experience in electrical power engineering. He has published around 100 research papers in refereed journals and conferences. He is leading multiple million projects in a capacity building funded by Erasmus+ with partners from Europe, Egypt, and Sri Lanka. In addition to projects funded by SFC and ETP, he is also working with power industry companies on development projects to assess their assets. His current research interests include artificial intelligence control applications in condition monitoring and control of FACTS. He organized and chaired the UPEC2018 Conference.

AHMED A. ABOUSHADY (Senior Member, IEEE) received the B.Sc. (Hons.) and M.Sc. degrees in electrical and control engineering from the Arab Academy for Science and Technology, Egypt, in 2005 and 2008, respectively, and the Ph.D. degree in power electronics from the University of Strathclyde, U.K., in 2013. He is currently a Senior Lecturer of power electronic systems with Glasgow Caledonian University, U.K. He has published several papers in refereed journals/conferences, textbooks, book chapters, and the PCT patent number PCT/GB2017/051364. His current research interests include DC–DC converters, high-voltage DC transmission systems, grid integration of renewable energy, and distributed generation systems.

SHERIF M. DABOUR (Senior Member, IEEE) received the B.Sc. degree in electrical engineering from Zagazig University, Egypt, in 2002, and the M.Sc. and Ph.D. degrees in electrical power engineering from Tanta University, Egypt, in 2012 and 2015, respectively.

He has extensive experience in research and academic teaching of electrical power and industrial electronics. From 2003 to 2009, he was a Lecturer and a Certified Trainer with Technical and Vocational Training Corporation, Riyadh, Saudi Arabia. In 2009, he joined Tanta University, where he is currently an Associate Professor (on academic leave). He has been involved in many projects funded by the Egyptian Academy of Scientific Research and Technology and the Qatar National Research Foundation. He is also a Researcher-1A with Glasgow Caledonian University, U.K., where he is participating in research funded by the British Council and Academy of Engineering and European Commission Projects. He has supervised the M.Sc. students and three Ph.D. students. To date, he has published 49 papers in international journals and conferences in the field of expertise. His current research interests include analysis, modeling, and application of power electronic converters. In addition, he studied wind turbines, PV systems, storage systems, microgrids, electric vehicle chargers, and energy storage integration. He served as a Treasurer for the Egypt Chapter of the IEEE Power Electronics Society (PELS), from 2017 to 2020. Additionally, he is a Reviewer of several journals, including IEEE TRANSACTIONS ON POWER ELECTRONICS AND INDUSTRIAL ELECTRONICS, *IET Power Applications*, and *IET Power Electronics*.